International Journal of Control
Publication details, including instructions for authors and subscription information:
http://www.tandfonline.com/loi/tcon20

Power-based control with integral action for wind turbines connected to the grid

R.R. Peña[a,b], R.D. Fernández[b], R.J. Mantz[c,d] & P.E. Battaiotto[c]

[a] Consejo Nacional de Investigaciones Científicas y Tecnológicas CONICET, La Plata, Argentina

[b] Departamento de Electrónica, Facultad de Ingeniería, Universidad Nacional de la Patagonia San Juan Bosco, Comodoro Rivadavia, Argentina

[c] LEICI, Facultad de Ingeniería, Universidad Nacional de La Plata, La Plata, Argentina

[d] Comisión de Investigaciones Científicas de la Provincia de Buenos Aires, La Plata, Argentina

Accepted author version posted online: 08 Apr 2015.Published online: 10 Jun 2015.

To cite this article: R.R. Peña, R.D. Fernández, R.J. Mantz & P.E. Battaiotto (2015): Power-based control with integral action for wind turbines connected to the grid, International Journal of Control, DOI: 10.1080/00207179.2015.1039064

To link to this article: http://dx.doi.org/10.1080/00207179.2015.1039064

International Journal of Control, 2015
http://dx.doi.org/10.1080/00207179.2015.1039064

Power-based control with integral action for wind turbines connected to the grid

R.R. Peña[a,b,*], R.D. Fernández[b], R.J. Mantz[c,d] and P.E. Battaiotto[c]

[a]*Consejo Nacional de Investigaciones Científicas y Tecnológicas CONICET, La Plata, Argentina;* [b]*Departamento de Electrónica, Facultad de Ingeniería, Universidad Nacional de la Patagonia San Juan Bosco, Comodoro Rivadavia, Argentina;* [c]*LEICI, Facultad de Ingeniería, Universidad Nacional de La Plata, La Plata, Argentina;* [d]*Comisión de Investigaciones Científicas de la Provincia de Buenos Aires, La Plata, Argentina*

(*Received 6 October 2014; accepted 5 April 2015*)

In this paper, a power shaping control with integral action is employed to control active and reactive powers of wind turbines connected to the grid. As it is well known, power shaping allows finding a Lyapunov function which ensures stability. In contrast to other passivity-based control theories, the power shaping controller design allows to use easily measurable variables, such as voltages and currents which simplify the physical interpretation and, therefore, the controller synthesis. The strategy proposed is evaluated in the context of severe operating conditions, such as abrupt changes in the wind speed and voltage drops.

Keywords: power shaping; passivity; integral control; renewable distributed generation; wind generation

1. Introduction

Renewable distributed generation (RDG) systems constitute a suitable alternative to increase the local supply of electricity. RDG covers a wide range of technologies for the generation of electrical energy (as wind turbines, solar cells, fuel cells) and storage systems (Lasseter, 2010).

The distributed generation systems have characteristics and behaviours difficult to predict (such as complex dynamics, failures, fluctuations in the load and the generation, etc.) with conventional tools of analysis and control. To cope with these constraints, new control strategies based on concepts of Lyapunov, passivity, robust control, etc. have been recently considered (Fernández, Battaiotto, & Mantz, 2010; Keyhani, Marwali, & Dai, 2009; Muhando, Senjyu, Uehara, & Funabashi, 2011; Ortega, Espinosa-Pérez, & Astolfi, 2013; Wang & Chen, 2005).

In this paper, we explore the application of the technique known as power shaping (PS) control, which has been proposed in Ortega, Jeltsema, and Scherpen (2003a, 2003b) and Jeltsema and Scherpen (2007). The PS control, as all the techniques derived from passivity concepts, does not require a linear model for achieving the control law. Other attractive characteristics are that the PS allows to obtain the corresponding domain of attraction and to establish a Lyapunov function for ensuring stability. In contrast to the interconnection and damping assignment control, the PS control is applicable to systems with pervasive dissipation, and also permits the use of equations considering variables as voltages and currents instead of charges and fluxes (García-Canseco, Jeltsema, Ortega, & Scherpen, 2010; García-Canseco, Ortega, Scherpen, & Jeltsema, 2007).

Recently, the PS control has been extended to include the integral and adaptive control (Dirksz & Scherpen, 2010). In this way, the robustness of the control system is increased and the steady-state error caused by unknown disturbances or by uncertainties in the model can be cancelled. Moreover, preserving the structure of the equations of Brayton–Moser, the good control properties of the PS are maintained by the addition of the integral control (Dirksz & Scherpen, 2012a).

In this paper, a PS-based integral control is applied to the control of a wind turbine in the RDG context. Particularly, with the aim of analysing the potential of this technique in the problems of RDG, PS controllers with integral action for the active and reactive powers are proposed. Wind turbine with rotor winding induction generators (DFIG) powered is considered. The system behaviour in the presence of voltage drops and wind speed changes is evaluated by simulation.

The paper is structured as follows. Section 2 introduces the basics to synthesise a controller using the technique PS-based integral control. Section 3 presents the dynamical system model and the development of the PS control proposed. Afterward, the proposal is evaluated in Section 4. Finally, the conclusions are summarised.

2. Power shaping control fundamentals

In this section, we summarise the PS stabilisation obtained in García-Canseco et al. (2007, 2010) and the PS control

*Corresponding author. Email: ramirop@unpata.edu.ar

with integral action presented in Dirksz and Scherpen (2010, 2012a), which are used in Section 3.2 for developing the control law for the wind turbine powers.

2.1 Power shaping stabilisation

Assume a dynamical system

$$\begin{cases} \dot{x} = f(x) + g(x)u \\ y = h(x) \end{cases}, \tag{1}$$

where $x \in \mathbb{R}^n$ is the state vector, $u \in \mathbb{R}^m$ is the input vector with $m \leq n$, $f(x) : \mathbb{R}^n \to \mathbb{R}^n$ and $g(x) : \mathbb{R}^n \to \mathbb{R}^n \text{x} \mathbb{R}^m$. The system (1) can be described employing the Brayton–Moser equations (García-Canseco et al., 2010)

$$Q(x)\dot{x} = \frac{\partial P(x)}{\partial x} + g(x)u, \tag{2}$$

where $Q : \mathbb{R}^n \to \mathbb{R}^{n\text{x}n}$ is a full rank matrix and $P(x)$ is a mixed-potential function.

According to García-Canseco et al. (2010) and García-Canseco et al. (2007), the following propositions are used to synthesise a stabilising controller by PS:

(1) There exist a full range matrix $\tilde{Q} : \mathbb{R}^n \to \mathbb{R}^{n\text{x}n}$, non-singular that solves the differential equation

$$\nabla(\tilde{Q}(x)f(x)) = [\nabla(\tilde{Q}(x)f(x))]^T, \tag{3}$$

and furthermore verifies that

$$\tilde{Q}(x) + \tilde{Q}(x)^T \leq 0. \tag{4}$$

(2) There is a scalar function $P_a : \mathbb{R}^n \to \mathbb{R}$, positive definite in the neighbourhood of an equilibrium point x^*, which verifies the following partial differential equation:

$$g^{\perp}(x)\tilde{Q}^{-1}(x)\nabla P_a(x) = 0, \tag{5}$$

where

$$g^{\perp}(x)g(x) = 0 \tag{6}$$

being

$$\text{rank}(g^{\perp}(x)) = n - m. \tag{7}$$

(3) The equilibrium point x^* is asymptotically stable, with a Lyapunov function $P_d(x)$, such that $(x^*) = \text{argmin} P_d(x)$, then the gradient and the Hessian of $P_d(x^*)$ are

$$\nabla P_d(x^*) = 0, \tag{8}$$

$$\nabla^2 P_d(x^*) > 0, \tag{9}$$

where the total power function is given by

$$P_d(x) = P(x) + P_a(x) \tag{10}$$

with

$$P(x) = \int [\tilde{Q}(x)f(x)]^T dx. \tag{11}$$

Under these conditions, the control law,

$$u_{PS} = [g^T \tilde{Q}^T \tilde{Q} g]^{-1} g^T \tilde{Q}^T \nabla P_a \tag{12}$$

guarantees a dynamical stability in the domain of attraction given by

$$\{x \in \mathbb{R}^n | P_d(x) \leq c\}, \tag{13}$$

with $c > 0$.

In contrast with the port-Hamiltonian framework, a practical advantage of the PS ones for electrical systems is that their dynamics can be described from variables, such as currents and voltages (Jeltsema & Scherpen, 2003) additionally allows to include dissipative elements in a natural way. On the other side, as a difference with the traditional techniques, PS is a nonlinear one that guarantees the convergence to the equilibrium point, by the Lyapunov function $P_d(x)$. Also, RDG systems are nonlinear and the application of conventional linear techniques (PI, PID) could not guarantee performance throughout the operating range. In this sense, the utilisation of advanced control techniques, such as the PS control or gain-scheduled $\mathcal{H}_\infty$ improve the whole behaviour (Muhando et al., 2011). Finally, the PS control, besides stability as in high-gain techniques, can improve the system performance by providing the freedom to choose different energy functions which, also, result in a clearer physical interpretation of the control action.

2.2 Power shaping control with integral action

It is well known the capability of controllers with integral action for compensating steady-state errors caused by disturbances or uncertainties in the model. In this way, to propose a PS control with integral action in closed-loop that retains the structure of the equations of Brayton–Moser only, constant disturbances satisfying the matching condition are considered. In the next paragraphs, the power-based integral control proposed in Dirksz and Scherpen (2010) and Dirksz and Scherpen (2012a) is summarised.

The equations of Brayton–Moser (2) can be written as

$$Q(x)\dot{x} = \frac{\partial P}{\partial x} + g(x)(u - d), \tag{14}$$

where d is the perturbation.

Then, the control action (Dirksz & Scherpen, 2010)

$$u = u_{PS} + \tau, \tag{15}$$

stabilises the system (14) asymptotically, being τ the integral state with dynamics

$$\dot{\tau} = -K_i g^T(x)\tilde{Q}^{-1}(x)\frac{\partial P_d(x)}{\partial x} \tag{16}$$

and

$$P_i(x) = P_d(x) + \frac{1}{2}\bar{\tau}^T K_i^{-1}\bar{\tau}, \tag{17}$$

the new Lyapunov function, with K_i a positive definite constant and $\bar{\tau} = \tau - d$. The proof of stability is accomplished using Lasalle's invariance principle being the domain of attraction given by the invariant set

$$\{(x, \bar{\tau}) \in \mathbb{R}^{n+m} | \tilde{P}_i(x, \bar{\tau}) \leq c_1\}, \tag{18}$$

with $c_1 > 0$.

3. Turbine powers controller design

3.1 System model

Figure 1 shows a doubly fed induction generator (DFIG) driven by a three-bladed horizontal axis wind turbine. They are coupled by a gearbox and a back-to-back converter between the rotor and the grid allows to control the generated power. This topology, widely used, is one of the most versatile wind conversion systems (Bianchi, De Battista, & Mantz, 2006; Miller, Sanchez-Gasca, Price, & Delmerico, 2003).

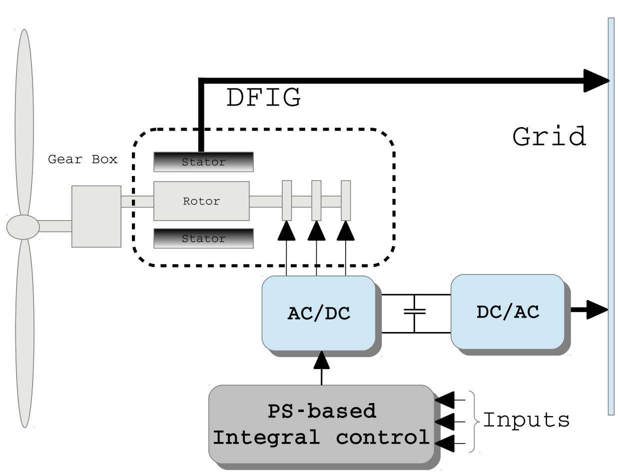

Figure 1. Wind conversion system connected to the electrical grid.

The stator and rotor voltages in the DFIG are (Wu, Lang, Zargari, & Kouro, 2011)

$$\vec{u_{sg}} = R_s\vec{i_{sg}} + \frac{d\vec{\lambda_{sg}}}{dt}, \tag{19}$$

$$\vec{u_{rg}} = R_r\vec{i_{rg}} + \frac{d\vec{\lambda_{rg}}}{dt}, \tag{20}$$

where R_s and R_r are the resistance of the stator and rotor windings, $\vec{\lambda_{sg}}$ and $\vec{\lambda_{rg}}$ are the stator and rotor flux-linkage vectors, $\vec{i_{sg}}$ and $\vec{i_{rg}}$ are the stator and rotor currents vectors. Expressing these in a generic rotating framework (x, y), the active and reactive powers can be written by

$$P_s = \frac{3}{2}(u_{sx}i_{sx} + u_{sy}i_{sy}), \tag{21}$$

$$Q_s = \frac{3}{2}(u_{sy}i_{sx} - u_{sx}i_{sy}), \tag{22}$$

where considering a particular framework, $u_{sx} = 0$, $u_{sy} = U$, the active and reactive powers can be controlled independently (Vas, 1998),

$$P_s = \frac{3}{2}(Ui_{sy}), \tag{23}$$

$$Q_s = \frac{3}{2}(Ui_{sx}). \tag{24}$$

Considering $R_s i_{sx} \approx 0$ and taking in mind that the stator dynamics is comparatively fast with respect to the other ones of the machine, the flux can be considered constant (Kundur, 1993), then

$$i_{sy} = -\frac{L_m}{L_s}i_{ry}, \tag{25}$$

$$i_{sx} = \frac{U - \omega L_m i_{rx}}{\omega L_s}, \tag{26}$$

where i_{rx} and i_{ry} are the rotor currents in the framework (x,y) and ω is the line frequency. The expressions for the derivative of the rotor currents in the generic framework (x,y) and the equations that represent the mechanic component of system are

$$\begin{cases} \dfrac{di_{rx}}{dt} = -\dfrac{R_r}{L_r}i_{rx} + \dfrac{1}{L_r}u_{rx}, \\ \dfrac{di_{ry}}{dt} = -\dfrac{R_r}{L_r}i_{ry} + \dfrac{1}{L_r}u_{ry}, \\ J\dfrac{d\omega_r}{dt} = T_e - T_m - B_r\omega_r. \end{cases} \tag{27}$$

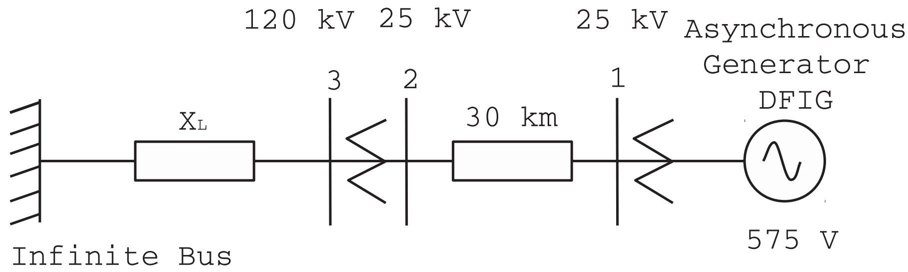

Figure 2. System analysed.

Furthermore, the developed electromagnetic torque is

$$T_e = \frac{3}{2} np(\lambda_{sx} i_{sy} - \lambda_{sy} i_{sx}), \tag{28}$$

being L_m the magnetising inductance, L_r the rotor self-inductance, L_s the stator self-inductance, u_{rx} and u_{ry} are the rotor voltages in the framework (x,y), T_m is the wind turbine mechanical torque, B_r is the combined coefficient of load friction and J is the inertia of the system, ω_r is the angular speed of the rotor and np is the number of pair of poles of the asynchronous generator.

3.2 Control design

From (27), the dynamical system can be written as

$$\begin{aligned} &f(x) + g(x)u \\ &= \begin{bmatrix} -\dfrac{R_r}{L_r} & 0 & 0 \\ 0 & -\dfrac{R_r}{L_r} & 0 \\ 0 & -\dfrac{B_r}{J} & -\dfrac{2B_r}{J} \end{bmatrix} \begin{bmatrix} x_1 \\ x_2 \\ x_3 \end{bmatrix} + \begin{bmatrix} 0 & \dfrac{1}{L_r} \\ \dfrac{1}{L_r} & 0 \\ 0 & 0 \end{bmatrix} u, \end{aligned} \tag{29}$$

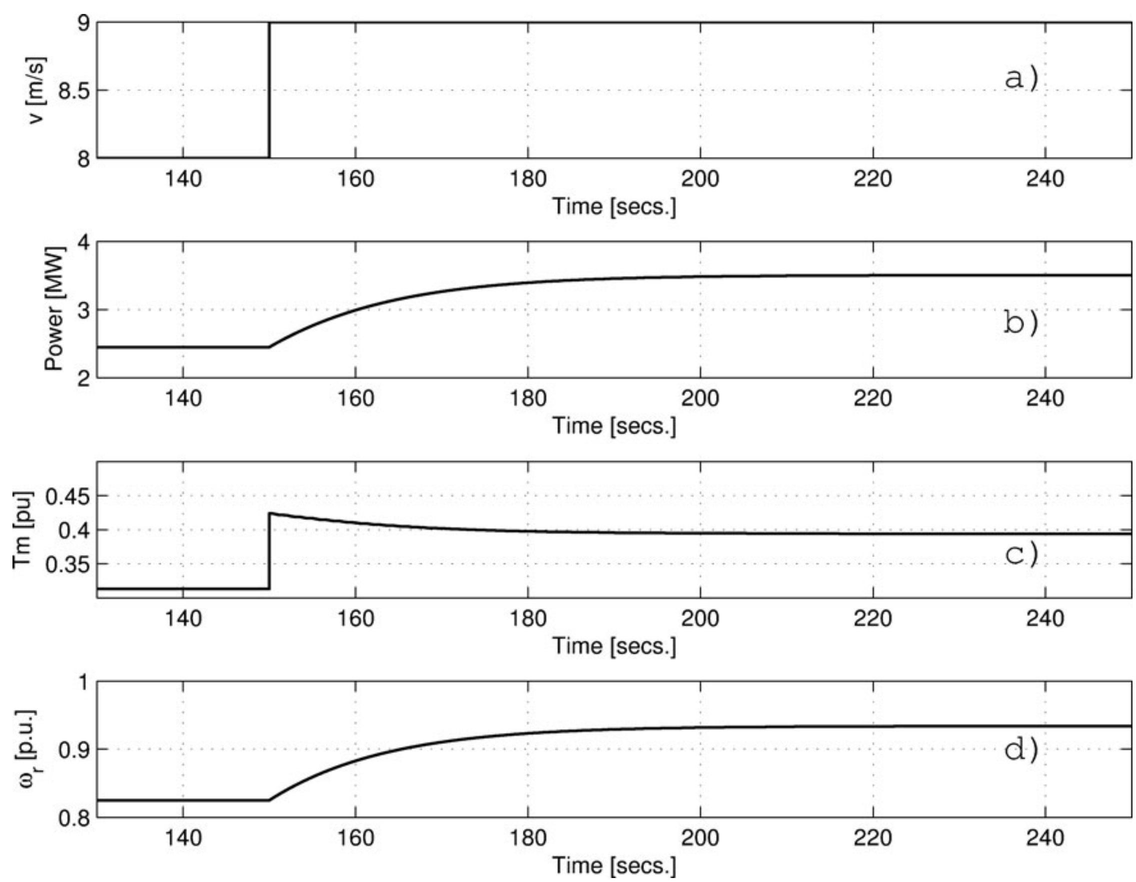

Figure 3. System analysed against a wind step. (a) Step in wind speed. (b) Active power. (c) Mechanical torque. (d) Shaft speed.

where the state variables x_1, x_2 are the currents i_{rx}, i_{ry} and x_3 is the rotor speed (ω_r). The system input vector is given by the voltages u_{rx} and u_{ry}. For purposes of controller design, the dynamics of converters can be neglected, since these may change the current very quickly, about half of electrical grid cycle (Peña, Clare, & Asher, 1996).

To synthesise two independent controllers for active and reactive powers, $g(x)$ is divided in

$$g_a(x) = \begin{bmatrix} 0 & 1/L_r & 0 \end{bmatrix}^T, \tag{30}$$

$$g_r(x) = \begin{bmatrix} 1/L_r & 0 & 0 \end{bmatrix}^T, \tag{31}$$

where $g_a(x)$ and $g_r(x)$ are the components of $g(x)$ for the active power control and the reactive power control, respectively.

Then, the control action using only the first term of Equation (15) is obtained evaluating (12)

$$u_P = \left(\frac{L_r q_{22}}{q_{22}^2 + q_{32}^2}\right)\frac{\partial P_{aP}(x)}{\partial x_2} + \left(\frac{L_r q_{32}}{q_{22}^2 + q_{32}^2}\right)\frac{\partial P_{aP}(x)}{\partial x_3}, \tag{32}$$

in an analogous way, the PS control action for the reactive power controller is

$$u_Q = \frac{L_r}{q_{11}}\frac{\partial P_{aQ}(x)}{\partial x_1}, \tag{33}$$

being q_{11}, q_{22} and q_{32} are the elements of the matrix $\tilde{Q}(x)$ presented in Appendix 1 and the function ($P_{aP}(x)$ and $P_{aQ}(x)$) employed for calculating (32) and (33) are presented in Appendix 2.

Then, according to (15) the complete expressions for the active and reactive powers controllers become

$$u_{FP} = \left(\frac{L_r q_{22}}{q_{22}^2 + q_{32}^2}\right)\frac{\partial P_{aP}(x)}{\partial x_2} + \left(\frac{L_r q_{32}}{q_{22}^2 + q_{32}^2}\right)\frac{\partial P_{aP}(x)}{\partial x_3} + \tau_a \tag{34}$$

and

$$u_{FQ} = \left(\frac{L_r}{q_{11}}\right)\frac{\partial P_{aQ}(x)}{\partial x_1} + \tau_r, \tag{35}$$

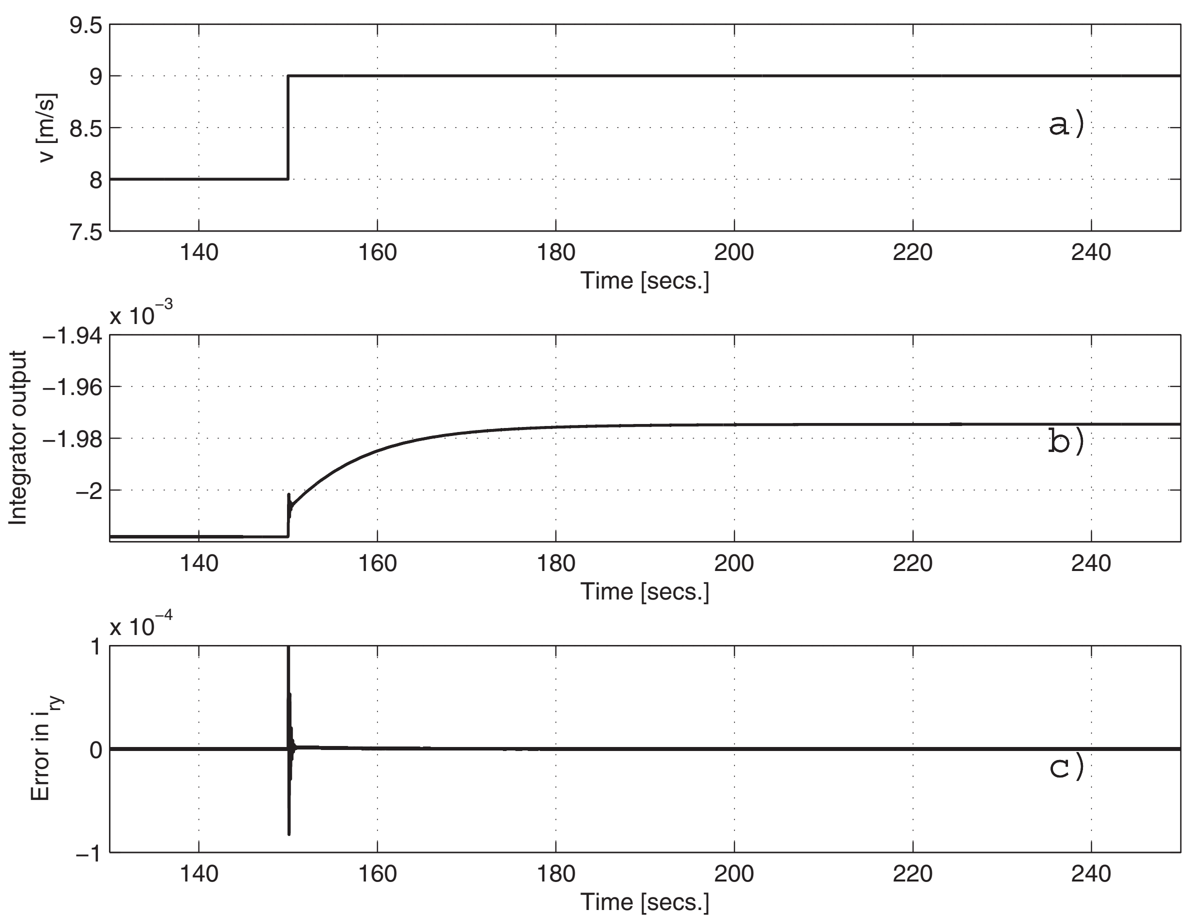

Figure 4. System analysed against a wind step. (a) Step in wind speed. (b) Integral action. (c) Error in i_{ry}; $(x_2 - x_2^*)$.

where the integral actions τ_a and τ_r are obtained from Equation (16), being their dynamics

$$\dot{\tau_a} = \left(-\frac{k_{ia}}{L_r q_{22}}\right)\frac{\partial P_d(x)}{\partial x_2} \tag{36}$$

and

$$\dot{\tau_r} = \left(-\frac{K_{ir}}{q_{11} L_r}\right)\frac{\partial P_d(x)}{\partial x_1}, \tag{37}$$

with $P_d(x)$ given by Equation (10), $K_{ia} > 0$ and $K_{ir} > 0$.

4. Simulation results

In this section, the controllers developed using concepts of power-based control with integral action are evaluated, considering a wind farm, with six turbines of 1.5 MW each one whose data are taken from Miller et al. (2003), connected to a power distribution system of 25 kV (Figure 2). The system exports power to a network of 120 kV through a line of 30 km. This topology has been used in several works for testing different control strategies (Evangelista, Valenciaga, & Puleston, 2012; Fernández, Mantz, & Battaiotto, 2010; López-García, Espinosa-Pérez, Siguerdidjane, & Dòria-Cerezo, 2013; Martinez, Tapia, Susperregui, & Camblong, 2012; Miller et al., 2003; Peña, Fernández, & Mantz, 2014).

In this work, reference torque for active power control is obtained from the optimum tracking curve

$$T_{\text{ref}}(\omega_r) = \frac{P_{\text{ref}}(\omega_r)}{\omega_r}, \tag{38}$$

which allows to extract the maximum power from the wind. The reference of power $P_{\text{ref}}(\omega_r)$ is obtain from Miller et al. (2003)

$$\omega_{\text{ref}} = -0.67P_{\text{ref}}^2 + 1.42P_{\text{ref}} + 0.51. \tag{39}$$

In the region of high winds, the goal is to limit the power captured by the wind turbine by pitching the wind turbine blades. This control is not considered in this work.

On the another hand, two strategies are considered for the reactive power control

- $Q_{\text{ref}} = 0$ (neutral to the grid).
- $Q_{\text{ref}} = f(U)$ (voltage regulation).

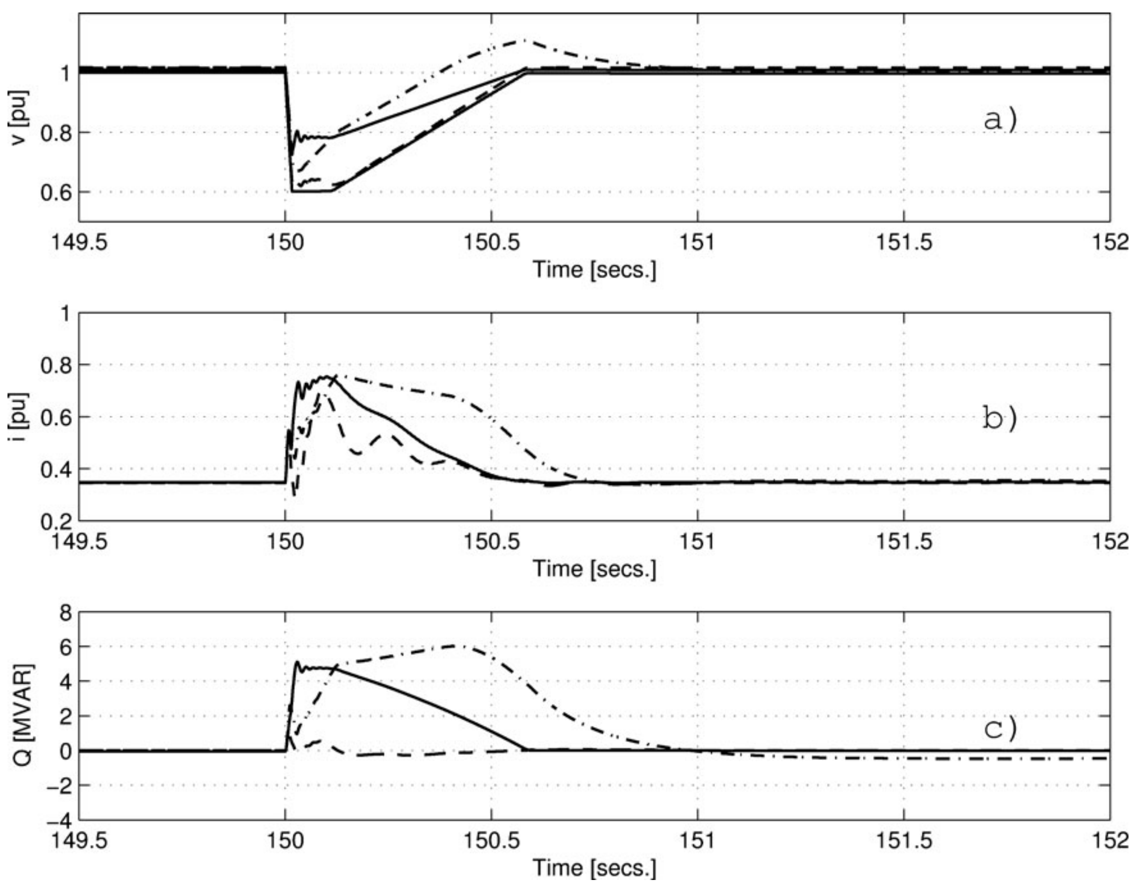

Figure 5. (a) Voltage in the infinite bus (solid line) and voltages in the connection point using CC, SC and PI strategies. (b) Currents injected by the wind farm and (c) Reactive powers in both cases.

From Equations (24) and (26), i_{rx} can be expressed as

$$i_{rx} = \frac{U^2 - (2/3)Q_s \omega L_s}{\omega L_m U}. \tag{40}$$

Then, the reference current is

$$i_{rx\mathrm{ref}} = \frac{U}{\omega L_m}. \tag{41}$$

For the second strategy (voltage regulation), we propose the following reference currents:

$$i_{rx\mathrm{ref}} = \left(\frac{U_{\mathrm{ref}} - U}{L_m \omega}\right) k_1 + k_2, \tag{42}$$

where U_{ref} is the reference voltage (1 pu), k_1 is an adjustment constant and k_2 ensures that the reactive power injected by the generator is zero when the voltage at the connection point is the nominal. The proportional control law (42) implies a reference current that tries to restore the voltage at the connection point increasing the reactive power injected to the grid.

Three cases are analysed for the purpose of demonstrating the feasibility of the active and reactive powers controllers (Equations (34) and (35)). In the first case, a step in wind speed is considered. Even though actual winds do not occur in this way, steps changes are commonly used as a standard testing signals because they permit a clear interpretation of the system behaviour against abrupt changes. Also, due to the harmonic contents, steps changes are much more demanding than real wind profiles.

Figure 3 consider this first case. In part (a) of this figure can be seen the step change in the wind velocity, which induces a variation of mechanical torque (Figure 3(c)), increasing the shaft speed (Figure 3(d)). The proposed controller forces the system to follow the reference given by Equation (38), increasing the power delivered to the grid as shown in Figure 3(b). It is important to note that meanwhile the turbine mechanical torque experiences a step due to the wind change, the generated electric power follows the reference given by the wind turbine speed. Both mechanical and electrical torques only coincide in steady state. The contribution of the integral term of the controller is shown in Figure 4(b), against the disturbance shown in Figure 4(a). The effect of integral control over i_{ry} (state x_2) is shown in Figure 4(c). As indicated in Figure 4(b), the integrator

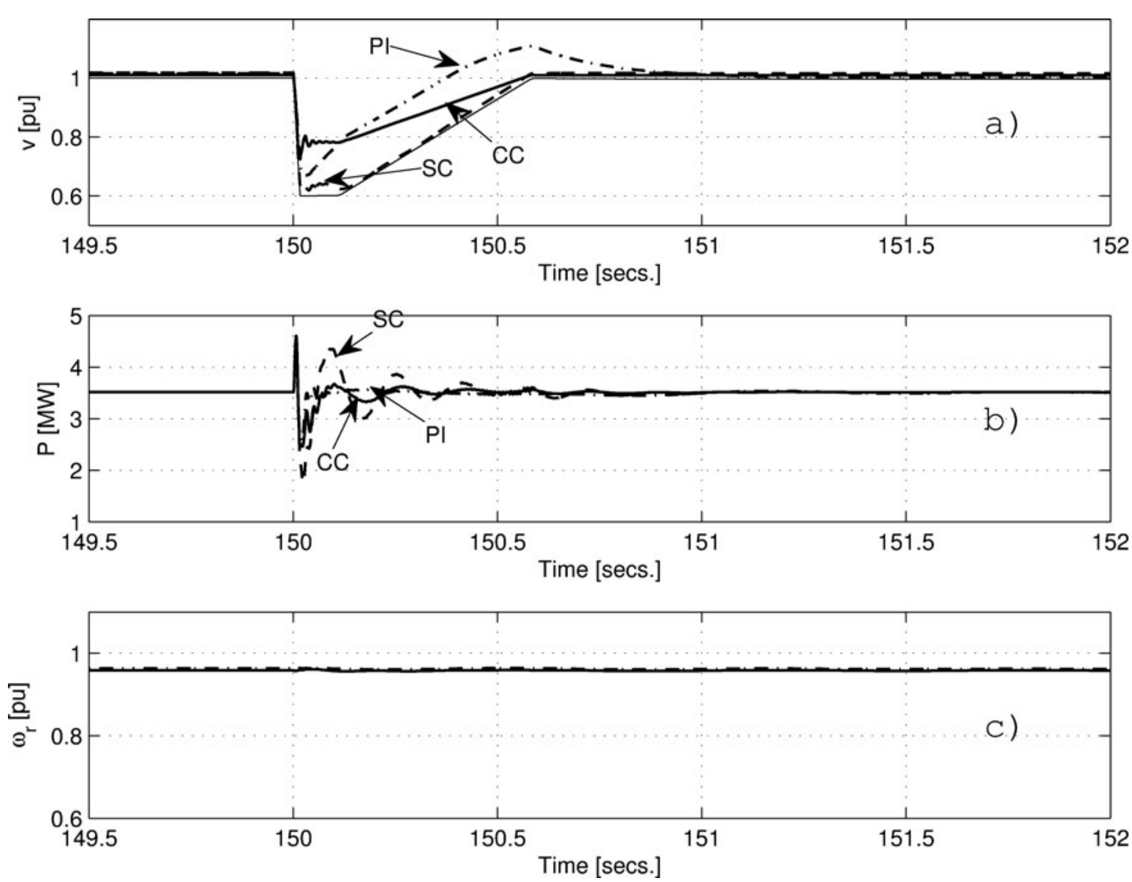

Figure 6. (a) Voltage in the infinite bus (solid line) and voltage in the connection point. (b) Active power. (c) Speed shaft.

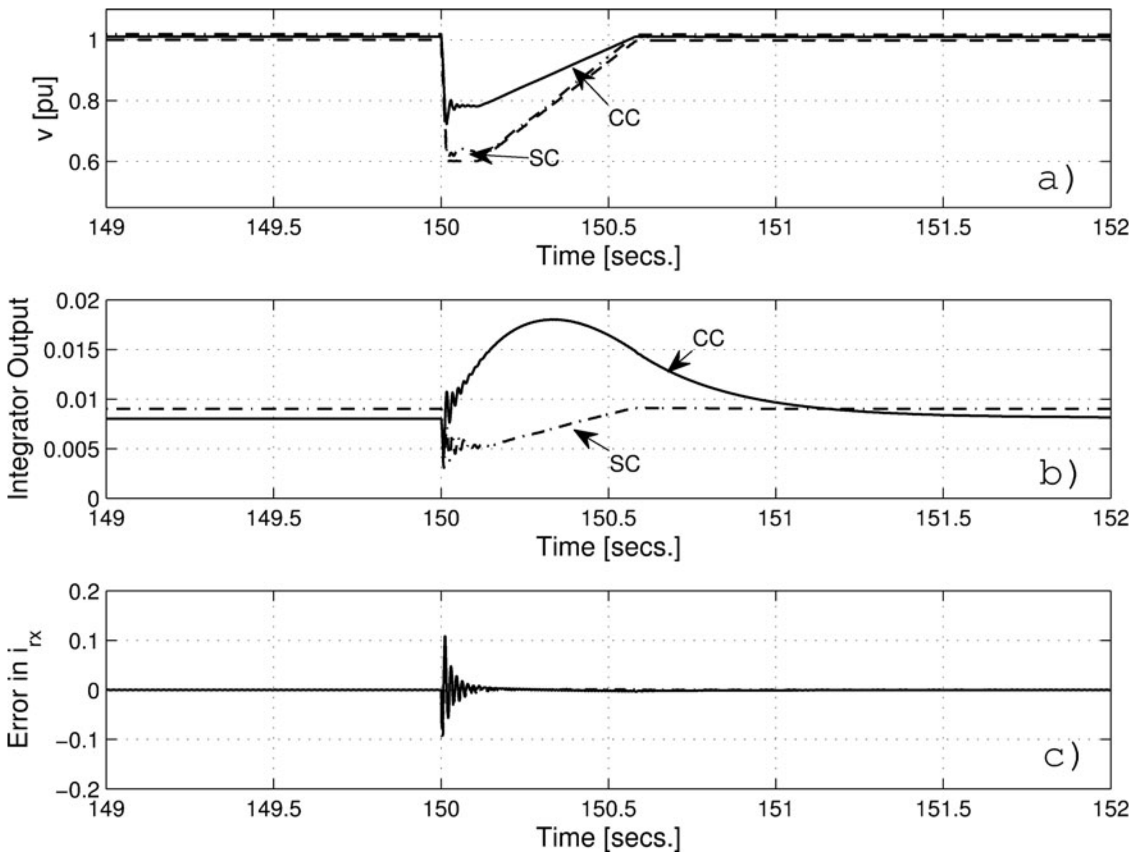

Figure 7. (a) Drop voltage in the infinite bus (dashed line) and voltage in the connection point. (b) Integrator output. (c) Error in i_{rx}; $(x_1^* - x_1)$.

output changes in order to maintain zero steady-state error over i_{ry}.

The second case considered is a voltage drop of 0.4 pu and 0.6 seconds in duration. This kind of failure is useful for evaluating the compliance of one of the new and more important requirement for grid connection of wind farms, which is fault ride-through capability, i.e. wind turbines must contribute to the electrical system in the event of failures, such as voltage drops (Ezzat, Benbouzid, Muyeen, & Harnefors, 2013; Piwko et al., 2010). Figure 5(a) shows voltages in the infinite bus (solid line) and at generator connection point in three situations: neutral reactive control ('SC'), expression (41), voltage control ('CC'), expression (42), and classical PI control ('PI') which is developed in Miller et al. (2003).

The currents delivered by the wind farm to the grid in 'SC', 'CC' and 'PI' cases can be observed in Figure 5(b). Before the voltage sag, the steady-state value of the current is such that the reactive power is null (Figure 5(c)). When strategies 'CC' and 'PI' are used, after failure, an increase in the current is detected (Figure 5(b)), which give place to a rise of the reactive power injected into the grid (Figure 5(c)). As a consequence, the voltage at the connection point is improved (Figure 5(a)).

By comparing the results of the three reactive control strategies, it is noted that the strategy for neutral contribution of reactive power to the grid presents a good performance for normal conditions. However, it does not contribute efficiently to restore the connection point voltage. Both strategies 'PI' and 'CC' inject reactive power to the electrical grid recovering the voltage at the connection point of the DFIG, Figure 5(a). At the beginning of the fault, due to the injection of reactive power, Figure 5(c), the 'PI' strategy is slower than the 'CC' one. Then, the voltage drop at the connection point is initially deeper in the 'PI' strategy which, also, presents an overshoot in the voltage when the failure is overcome (Figure 5(a)). Furthermore, after the fault is overcome, the reactive power in the 'PI' strategy slowly recovers its steady-state value (Figure 5(c)).

Figure 6 shows the performance of the active power controller in presence of the voltage drop in the infinite bus. For clarity, Figure 5(a) is repeated in Figure 6(a). In Figure 6(b) can be seen the active power contribution, particularly how the power is restored after failure was exceeded. In Figure 6(c), a small variation of the speed of the shaft in relation to the magnitude of the failure is observed. The voltage at the connection point is restored after the fault is overcome (Figures 5(a) and 6(a)).

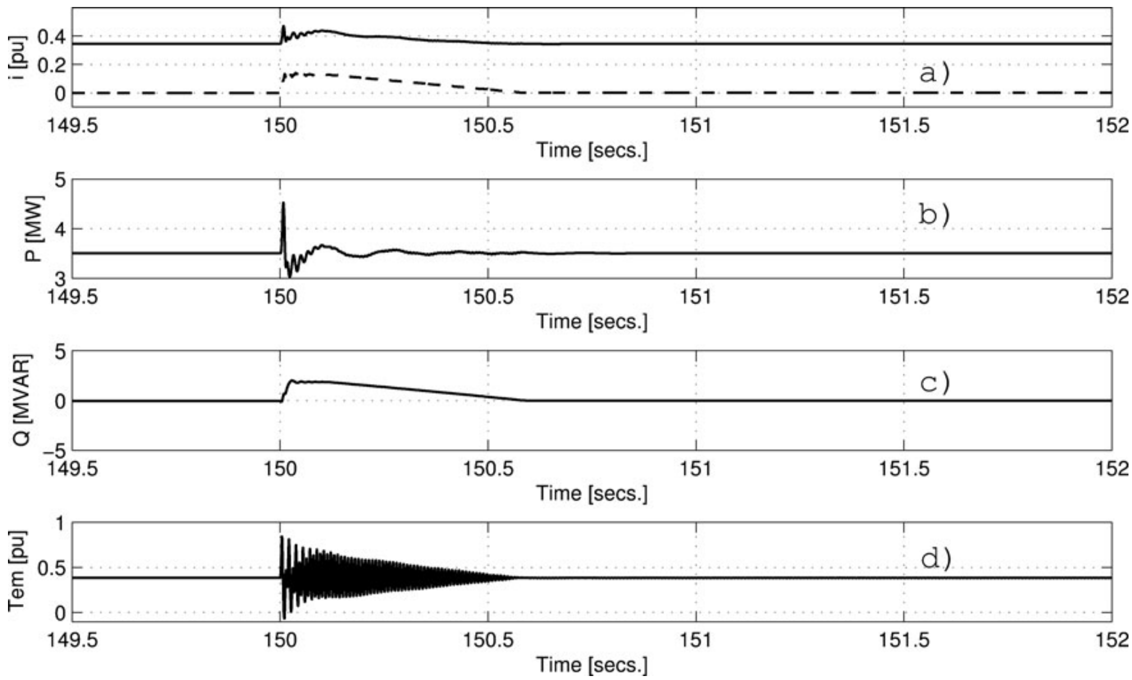

Figure 8. (a) Positive sequence current (solid line) and negative sequence current (dashed line) in the connection point. (b) Active power. (c) Reactive power. (d) Electromagnetic torque.

The effect of the integral control on the variable i_{rx} is shown in Figure 7. In part (b) of Figure 7, the contribution of the integral control is shown, which allows to achieve zero steady-state error (Figure 7(c)).

The third case considered is an unbalanced voltage drop of 0.4 pu and 0.6 seconds for the 'CC' strategy. When the system is balanced, current in the DFIG, there is only positive sequence, if an imbalance occurs, there is a negative sequence current (Leon, Mauricio, & Solsona, 2012; Martinez, Tapia, Susperregui, & Camblong, 2011).

Figure 8(a) shows positive and negative sequences current in solid and dashed line, respectively. In Figure 8(b) and 8(c), active and reactive powers are presented. Finally, Figure 8(d) shows the behaviour of the electromagnetic torque against the unbalanced voltage drop.

5. Conclusion

This work analyses the use of PS concepts. A new approach of the passivity-based control theory is employed to synthesise two decoupled controllers for the active and reactive powers of a wind turbine connected to an electrical grid. Particularly, PS controllers with integral actions are designed, which by preserving the structure of the equations of Brayton–Moser, allows to maintain the known properties of the classical power-based control.

The proposed control strategies were evaluated for severe events, such as sudden changes in the wind speed, a strong voltage drop and a unbalanced voltage drop.

Two cases were considered for the reactive power control, the neutral contribution to the grid and the voltage regulation at the connection point. The PS-based integral controllers worked properly in both cases. Specially, the addition of the voltage control shows a better performance in the presence of a voltage drop.

Further studies about mitigation of an unbalanced grid voltage condition using the PS control will be studied in future works.

The first results are promising and encourage to extend the field of application of the PS design in more complex RDG systems.

Acknowledgements

This work has been performed through CONICET, UNPSJB, UNLP, CICpBA.

Disclosure statement

No potential conflict of interest was reported by the authors.

References

Bianchi, F.D., De Battista, H., & Mantz, R.J. (2006). *Wind turbine control systems: Principles, modelling and gain scheduling design*. London: Springer-Verlag London Ltd.

Dirksz, D.A., & Scherpen, J.M.A. (2010). Power-based adaptive and integral control of standard mechanical systems. In *2010 49th IEEE Conference on Decision and Control* (pp. 4612–4617). Atlanta, GA: IEEE.

Dirksz, D.A., & Scherpen, J.M.A. (2012a). Power-based control: Canonical coordinate transformations, integral and adaptive control. *Automatica, 48*(6), 1045–1056.

Dirksz, D.A., & Scherpen, J.M.A. (2012b). Power-based setpoint control: Experimental results on a planar manipulator. *IEEE Transactions on Control Systems Technology, 20*(5), 1384–1391.

Evangelista, C., Valenciaga, F., & Puleston, P. (2012). Multivariable 2-sliding mode control for a wind energy system based on a double fed induction generator. *International Journal of Hydrogen Energy, 37*(13), 10070–10075.

Ezzat, M., Benbouzid, M., Muyeen, S.M., & Harnefors, L. (2013). Low-voltage ride-through techniques for DFIG-based wind turbines: State-of-the-art review and future trends. In *39th Annual Conference of the IEEE Industrial Electronics Society* (pp. 7681–7686). Vienna: IEEE.

Fernández, R., Battaiotto, P., & Mantz, R. (2010). Wind farm control based on passivity. In *2010 IEEE International Conference on Industrial Technology* (pp. 1000–1005). Vina del Mar: IEEE.

Fernández, R., Mantz, R., & Battaiotto, P. (2010). Linear and non-linear control of wind farms. Contribution to the grid stability. *International Journal of Hydrogen Energy, 35*(11), 6019–6024.

García-Canseco, E., Jeltsema, D., Ortega, R., & Scherpen, J.M. (2010). Power-based control of physical systems. *Automatica, 46*(1), 127–132.

García-Canseco, E., Ortega, R., Scherpen, J.M.A., & Jeltsema, D. (2007). Power shaping control of nonlinear systems: A benchmark example. *Lecture Notes in Control and Information Sciences* (366), 135–146.

Jeltsema, D. (2005). *Modeling and control of nonlinear networks: A power-based perspective*. Netherlands: Delft University of Technology.

Jeltsema, D., & Scherpen, J.M.A. (2003). A dual relation between port-Hamiltonian systems and the Brayton–Moser equations for nonlinear switched RLC circuits. *Automatica, 39*(6), 969–979.

Jeltsema, D., & Scherpen, J.M.A. (2007). A power-based description of standard mechanical systems. *Systems and Control Letters, 56*(5), 349–356.

Keyhani, A., Marwali, M.N., & Dai, M. (2009). *Integration of green and renewable energy in electric power systems*. Hoboken, NJ: Wiley.

Kundur, P. (1993). *Power systems stability and control*. New York, NY: McGraw-Hill.

Lasseter, R.H. (2010). Microgrids and distributed generation. *Intelligent Automation and Soft Computing, 16*(2), 225–234.

Leon, A., Mauricio, J., & Solsona, J. (2012). Fault ride-through enhancement of DFIG-based wind generation considering unbalanced and distorted conditions. *IEEE Transactions on Energy Conversion, 27*(3), 775–783.

López-García, I., Espinosa-Pérez, G., Siguerdidjane, H., & Dòria-Cerezo, A. (2013). On the passivity-based power control of a doubly-fed induction machine. *International Journal of Electrical Power & Energy Systems, 45*(1), 303–312.

Martinez, M., Tapia, G., Susperregui, A., & Camblong, H. (2011). DFIG power generation capability and feasibility regions under unbalanced grid voltage conditions. *IEEE Transactions on Energy Conversion, 26*(4), 1051–1062.

Martinez, M., Tapia, G., Susperregui, A., & Camblong, H. (2012). Sliding-mode control for DFIG rotor- and grid-side converters under unbalanced and harmonically distorted grid voltage. *IEEE Transactions on Energy Conversion, 27*(2), 328–339.

Miller, N., Sanchez-Gasca, J.J., Price, W., & Delmerico, R. (2003). Dynamic modeling of GE 1.5 and 3.6 MW wind turbine-generators for stability simulations. *IEEE Power Engineering Society General Meeting, 3*, 1977–1983.

Muhando, E., Senjyu, T., Uehara, A., & Funabashi, T. (2011). Gain-scheduled $\mathcal{H}_\infty$ control for WECS via LMI techniques and parametrically dependent feedback part I: Model development fundamentals. *IEEE Transactions on Industrial Electronics, 58*(1), 48–56.

Ortega, R., Espinosa-Pérez, G., & Astolfi, A. (2013). Passivity-based control of AC drives: Theory for the user and application examples. *International Journal of Control, 86*(4), 625–635.

Ortega, R., Jeltsema, D., & Scherpen, J.M.A. (2003a). Power shaping: A new paradigm for stabilization of nonlinear RLC circuits. *IEEE Transactions on Automatic Control, 48*(10), 1762–1767.

Ortega, R., Jeltsema, D., & Scherpen, J.M.A. (2003b). Stabilization of nonlinear RLC circuits: Power shaping and passivation. In *Proceeding of the 42nd IEEE Conference on Decision and Control* (pp. 5597–5602). Maui, HI: IEEE.

Peña, R., Clare, J., & Asher, G. (1996). Doubly fed induction generator using back-to-back PWM converters and its application to variable-speed wind-energy generation. *IEE Proceedings Electric Power Applications, 143*(3), 231–241.

Peña, R., Fernández, R., & Mantz, R. (2014). Passivity control via power shaping of a wind turbine in a dispersed network. *International Journal of Hydrogen Energy, 39*(16), 8846–8851.

Piwko, R., Miller, N., Girad, R., MacDowell, J., Clark, K., & Murdoch, A. (2010). Generator fault tolerance and grid codes. *IEEE Power and Energy Magazine, 8*(2), 18–26.

Vas, P. (1998). *Sensorless vector and direct torque control.* Oxford/New York: Oxford University Press.

Wang, W.J., & Chen, J.Y. (2005). Passivity-based sliding mode position control for induction motor drives. *IEEE Transactions on Energy Conversion, 20*(2), 316–321.

Wu, B., Lang, Y., Zargari, N., & Kouro, S. (2011). *Power conversion and control of wind energy systems*. Hoboken, NJ: Wiley-IEEE Press.

Appendix 1. Matrix $\tilde{Q}$

The matrix $\tilde{Q}(x)$ is proposed from the system of equation (3) and proposition (4)

$$\tilde{Q}(x) = \begin{bmatrix} q_{11} & 0 & 0 \\ 0 & q_{22} & 0 \\ 0 & q_{32} & q_{33} \end{bmatrix}, \tag{A1}$$

whose elements are

$$q_{11} = -1, q_{32} = \frac{3UL_mL_r}{J\omega L_s R_r}, q_{22} = -\frac{q_{32}^2}{3}, q_{33} = -1. \tag{A2}$$

where checking the principal minors of $\tilde{Q}(x) + \tilde{Q}(x)^T$, we can verify that $\tilde{Q}(x) + \tilde{Q}(x)^T < 0$.

For more complex systems, the matrix $\tilde{Q}(x)$ can be chosen from the procedure proposed in Jeltsema (2005), García-Canseco et al. (2007) and Dirksz and Scherpen (2012b).

Appendix 2. $P_{aP}(x)$ and $P_{aQ}(x)$ determination

For the determination of $P_{aP}(x)$ and $P_{aQ}(x)$, two annihilators are proposed such that (6) and (7) are verified. Then, evaluating Equation (5) becomes

$$g_P^{\perp}\tilde{Q}^{-1}\nabla P_{aP} = \begin{bmatrix} \frac{1}{q_{11}} & 0 & 0 \\ 0 & \frac{-q_{32}}{q_{22}q_{33}} & \frac{1}{q_{33}} \end{bmatrix} \nabla P_{aP} = 0, \tag{B1}$$

$$g_Q^{\perp}\tilde{Q}^{-1}\nabla P_{aQ} = \begin{bmatrix} 0 & \frac{1}{q_{22}} & 0 \\ 0 & \frac{-q_{32}}{q_{22}q_{33}} & \frac{1}{q_{33}} \end{bmatrix} \nabla P_{aQ} = 0. \tag{B2}$$

From Equation (B1)

$$-\frac{\partial P_{aP}(x)}{\partial x_1} = 0 \tag{B3}$$

and

$$-\frac{q_{32}}{q_{22}q_{33}}\left(\frac{\partial P_{aP}(x)}{\partial x_2}\right) + \frac{1}{q_{33}}\left(\frac{\partial P_{aP}(x)}{\partial x_3}\right) = 0, \tag{B4}$$

where Equation (B3) indicates that $P_{aP}(x)$ cannot depend on x_1. The second Equation (B4) is a partial differential equation (PDE) whose solution can be resolved by using a computer algebra system software and is given by a function Ψ_P. We fix $P_{aP}(x) = \Psi_P(x_2, x_3)$ where $\Psi_P : \mathbb{R}^2 \to \mathbb{R}$ is an arbitrary differentiable function such that $P_d(x) = P(x) + P_{aP}(x_2, x_3)$ has a minimum at x^* (García-Canseco et al., 2010). On the other hand, from Equation (B2)

$$\frac{1}{q_{22}}\left(\frac{\partial P_{aQ}(x)}{\partial x_2}\right) = 0, \tag{B5}$$

$$\frac{-q_{32}}{q_{22}q_{33}}\left(\frac{\partial P_{aQ}(x)}{\partial x_2}\right) + \frac{1}{q_{33}}\left(\frac{\partial P_{aQ}(x)}{\partial x_3}\right) = 0, \tag{B6}$$

then $P_{aQ}(x) = \Psi_Q(x_1)$ is fixed.

One possibility is to achieve (8) and (9) simultaneously is to select $P_{aP}(x)$ and $P_{aQ}(x)$ of the form

$$P_{aP}(x) = k_a(z - z^*)^2 + k_b(z - z^*), \tag{B7}$$

where

$$\begin{aligned} z &= -\frac{k_2}{k_1}x_2 + x_3, \\ z^* &= -\frac{k_2}{k_1}x_2^* + x_3^*, \\ k_b &= \frac{R_r q_{32}}{L_r}x_2^*, k_a = 1, k_1 = \frac{-q_{32}}{q_{22}q_{33}}, k_2 = \frac{1}{q_{33}} \end{aligned} \tag{B8}$$

and

$$P_{aQ}(x) = (z_1 - z_1^*) + (z_1 - z_1^*)^2 \tag{B9}$$

with

$$\begin{aligned} z_1 &= c_2 x_1, z_1^* = c_2 x_1^*. \\ c_2 &= \frac{q_{11}R_r}{2L_r}. \end{aligned} \tag{B10}$$